Plant and Cell Physiology Advance Access published January 28, 2015

PCP
PLANT & CELL PHYSIOLOGY

Special Focus Issue – Regular Paper

A Mathematical Model of Phloem Sucrose Transport as a New Tool for Designing Rice Panicle Structure for High Grain Yield

Motohide Seki[1,*], François Gabriel Feugier[1], Xian-Jun Song[2], Motoyuki Ashikari[2], Haruka Nakamura[3], Keiki Ishiyama[3], Tomoyuki Yamaya[3], Mayuko Inari-Ikeda[2], Hidemi Kitano[2] and Akiko Satake[1]
[1]Faculty of Environmental Earth Science, Hokkaido University, N10W5, Kita-ku, Sapporo, 060-0810 Japan
[2]Bioscience and Biotechnology Center, Nagoya University, Furo-cho, Chikusa-ku, Nagoya, 464-8601 Japan
[3]Graduate School of Agricultural Science, Tohoku University, 1-1 Tsutsumidori-Amamiyamachi, Aoba-ku, Sendai, 981-8555 Japan
*Corresponding author: E-mail, seki@ees.hokudai.ac.jp; Fax, +81-11-706–4954.
(Received July 22, 2014; Accepted November 21, 2014)

Rice (*Oryza sativa*) is one of the most important food crops in the world. Numerous quantitative trait loci or genes controlling panicle architecture have been identified to increase grain yield. Yet grain yield, defined as the product of the number of well-ripened grains and their weight, is a complex trait that is determined by multiple factors such as source, sink and translocation capacity. Mechanistic modelling capturing capacities of source, sink and transport will help in the theoretical design of crop ideotypes that guarantee high grain yield. Here we present a mathematical model simulating sucrose transport and grain growth within a complex phloem network. The model predicts that the optimal panicle structure for high yield shows a simple grain arrangement with few higher order branches. In addition, numerical analyses revealed that inefficient delivery of carbon to panicles with higher order branches prevails regardless of source capacity, indicating the importance of designing grain arrangement and phloem structure. Our model highlights the previously unexplored effect of grain arrangement on the yield, and provides numerical solutions for optimal panicle structure under various source and sink capacities.

Keywords: Breeding • Crop ideotype • Hagen–Poiseuille equation • Murray's law • *Oryza sativa* • Pressure–flow hypothesis.

Abbreviations: QTL, quantitative trait locus.

Introduction

To meet the increasing demand of food security, improving crop productivity through efficient breeding is an urgent task. Among staple cereal crops, rice is the most important crop in Asia, and recently its importance has been increasing in African and Latin American countries. Genetic and molecular studies in rice, as a monocot model plant, are well advanced, providing powerful tools for investigating the molecular bases of grain yield regulation and facilitating molecular breeding strategy.

Many quantitative trait loci (QTLs) and some genes controlling yield traits have been identified in the Asian domesticated species *Oryza sativa* (Sakai et al. 2013). Most of these are associated with a change in the sink capacity determined by the number and maximum size of grains. *Gn1a*, *APO1* and *TAW1* are known to affect numbers of spikelets (Ashikari et al. 2005, Huang et al. 2009, Wang et al. 2009, Terao et al. 2010, Yoshida et al. 2013), and *GS3*, *GW2* and *qSW5* (*GW5*) affect grain size by controlling grain length or width (Wan et al. 2006, Fan et al. 2006, Song et al. 2007, Shomura et al. 2008). As a result, cultivars with more or larger spikelets per panicle have become available (Peng et al. 2008). However, cultivars with large grain number often exhibit poor grain filling (slow grain-filling rate or many unfilled grains), exhibiting a clear trade-off between grain number and grain filling (Peng et al. 1999, Nagata et al. 2002, Yang and Zhang 2010). This trade-off is expected to reduce the grain yield appreciably because the yield is determined by the product of grain number per unit area and grain weight, which is directly influenced by grain filling. For this reason, understanding the mechanism underlying the emergence of trade-offs and designing cultivars that remedy the trade-offs are required to increase the grain yield.

The trade-off between grain number and grain filling is determined by multiple processes, including source limitation (shortage of assimilated carbon supply to panicle sinks), sink limitation (inability of each grain to unload and/or accumulate assimilated carbons; Ma et al. 1990) and translocation limitation (inefficient delivery of assimilated carbons from leaves to panicle sink). Partial grain removal experiments have shown that grains positioned in parts where inferior spikelets are frequently observed can be fully filled if some of the other grains are removed, indicating an effect of source limitation (Kato 2004, Ohsumi et al. 2011). Evidence of sink limitation has also been reported in studies showing that activities of enzymes associated with starch synthesis are weaker in inferior spikelets than in superior spikelets (Umemoto et al. 1994, Liang et al. 2001), and in studies isolating the gene regulating sucrose unloading during grain development (Wang et al. 2008). In other studies, a simultaneous increase in sink size and translocation capacity with increased number of vascular bundles contributed strongly to increased grain yield, with a lower reducing effect, or even an improved effect, on grain filling (*HI1* allele of *APO1*; Terao et al. 2010, *SPIKE*; Fujita et al. 2013). These findings indicate that the trade-off results from the complex interaction of source, sink and translocation capacities. Given

Plant Cell Physiol. 0(0): 1–15 doi:10.1093/pcp/pcu191, Advance Access publication on 15 December 2014, available online at www.pcp.oxfordjournals.org

the complexity of interactions that are involved in the determination of grain yield, schematic and intuitive models are not sufficient to describe them. Quantitative and integrative mathematical models are essential. Such mathematical models would be useful for theoretically designing crop ideotypes that guarantee high grain yield before any yield improvement breeding is performed (Donald 1968).

Here, we present a mechanistic model that integrates the processes of carbon assimilation in source leaves, sucrose translocation via a phloem network and carbon accumulation in sink grains, and we predict sucrose transport in phloem and position-dependent grain growth in a complex panicle structure. In this model, source and sink capacities are incorporated as external parameters that can be arbitrarily defined, whereas translocation capacity is intrinsic to the phloem network structure and of major interest. The purpose of this study was to identify an ideal panicle structure maximizing grain yield given source and sink capacities using our model. For this purpose, we performed the following analyses: (i) we determined the unknown structure of the phloem network using pipe or aorta models that have been used for the xylem system (McCulloh et al. 2003); (ii) we compared the predicted and observed grain growth patterns to test the validity of each model; (iii) using a model that could reproduce the observed data, we designed a panicle structure that maximized grain yield, and (iv) given the panicle structure, we calculated the maximum number of grains that can be fully developed during grain filling.

Crop models such as STICS (Brisson et al. 2003) and FSPM (Vos et al. 2010) have been widely used to predict crop growth and yield. In these models, the movement of assimilate is often described as a transfer coefficient, and a method for calculating the coefficient from the phloem anatomy has been developed (Sheehy et al. 1995) based on the widely accepted pressure–flow hypothesis (Münch 1930). Mechanistic models of phloem transport in a one-source and one-sink system (Dewar 1993, Thompson and Holbrook 2003a, Thompson and Holbrook 2003b, Thompson and Holbrook 2004, Hölttä et al. 2006, Hölttä et al. 2009), a one-source and two-sink system (Minchin et al. 1993) and a system with multiple sinks and sources (Daudet et al. 2002, Lacointe and Minchin 2008) have been proposed. These models have supported the validity of the pressure–flow hypothesis proposed by Münch (1930). Source–sink interactions in a dynamically growing architecture have been modeled using an electrical circuit analogy (Allen et al. 2005). However, no studies have applied such mechanistic models to investigate yield maximization in rice plants.

Phloem structure within a branched panicle should be specified in the mechanistic model on transport of assimilate from leaves to a panicle. Relatively few studies explored phloem structure in rice (e.g. Nakamura and Hoshikawa 1985). On the other hand, many theoretical studies have considered development of the whole plant structure (e.g. Stein and Boyer 2006), some of which can be helpful to model the unknown phloem structure within a branched panicle. In addition, from the viewpoint of optimal strategy theory, plant structure designed to maximize its fitness has been favored in the course of evolution. It follows that we can expect that the sieve tube is not very different from the optimal structure that maximizes transport efficiency. In the present study, we referred to studies of general physics on optimal network (Durand 2006) to specify phloem structure.

The model presented in this study allows simulation of sucrose translocation within the complex phloem network of rice panicles, a capability that is useful for identifying an ideal panicle structure maximizing grain yield. Our study highlights the previously unexplored role of grain arrangements in determining grain yield and proposes the ideal panicle as the simplest branching network structure bearing no branches of higher order than secondary. Accompanied by modern breeding techniques, a computational approach will be increasingly useful for next-generation breeding strategies aimed at obtaining high-yielding cultivars.

Results

Modeling panicle structure and phloem network

The rice panicle consists of a panicle rachis (main axis) and primary, secondary and higher order branches (**Fig. 1A**). In the present model, we consider a phloem network where each of the *M* spikelets (the sink organs) and a single set of leaves (the source) are connected by a sieve tube (**Fig. 1B**; see the Materials and Methods for details).

In the panicle of *japonica* cultivars, each of the several large vascular bundles containing multiple sieve tubes is assigned to a primary branch at each branching point of the rachis (Hoshikawa 1989; **Fig. 2A, B**); thus, the number of large vascular bundles and primary branches is the same. In the primary and higher order branches, little is known about how each sieve tube in the large vascular bundle is distributed in the phloem network and whether each sieve tube bifurcates into daughter tubes. We developed two very different models, pipe and aorta models, to determine the structure of the phloem network in rice panicles and to identify the model most appropriate for explaining actual grain growth.

The pipe model, originally proposed by Shinozaki et al. (1964a, 1964b), considers that each sieve tube is independent and that there is no exchange of solution between them at any location (**Fig. 2A**). An essential assumption of the pipe model is that each pipe neither bifurcates nor tapers. In contrast, a network in which a single tube bifurcates into multiple daughter tubes is called an aorta model, named after the blood vessel system in animals (McCulloh et al. 2003). In the aorta model, we approximated several sieve tubes in each large vascular bundle by a single large tube per bundle (**Fig. 2B**). One large sieve tube is assigned to one primary branch, and the mother tube bifurcates into two daughter tubes at each branching point, which we call a junction (**Figs. 1B**, **2C**). We assume that every bifurcation obeys Murray's law, stating that the cubic radius of the mother tube is equal to the sum of the cubic radii of the two daughter tubes (thus, neither daughter tube is ever thicker than its mother tube). The two daughter tubes may have different radii, giving asymmetric branching, which is decided by the key parameter σ ($1/2 < \sigma < 1$; **Fig. 2C**). When $\sigma = 1/2$, the two

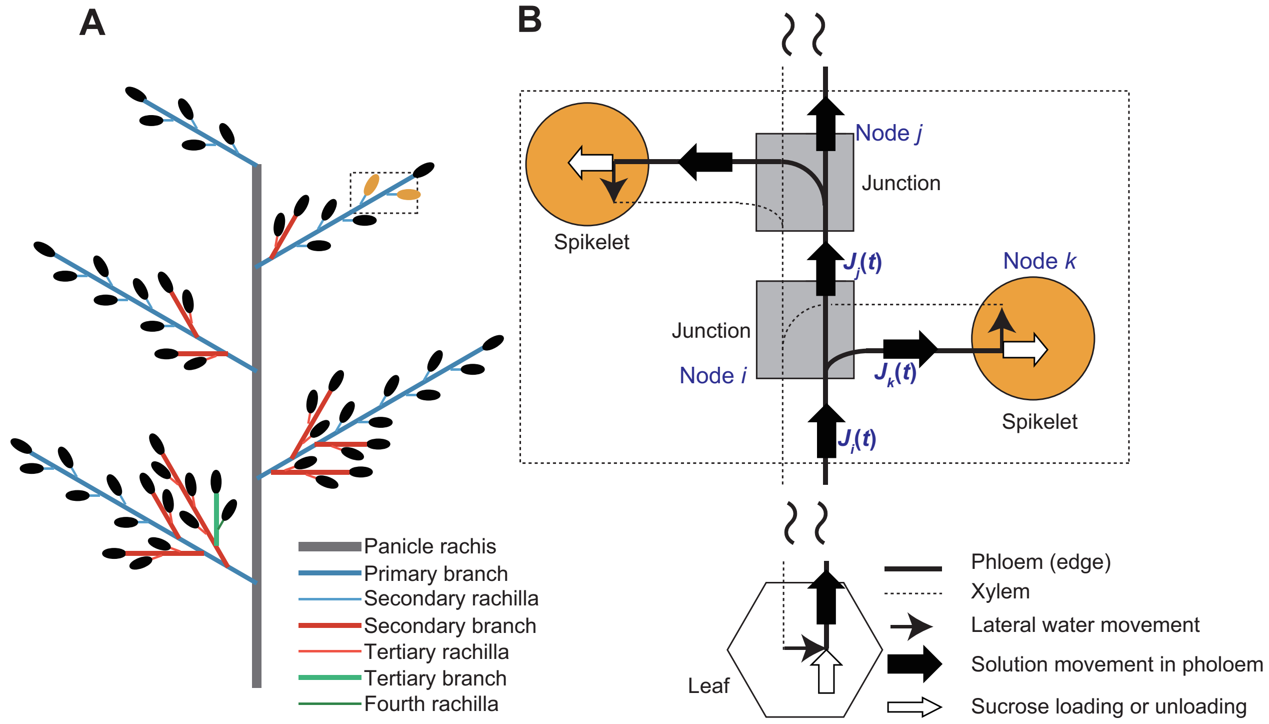

Fig. 1 Schematics of a sucrose transport model in the phloem network of a rice panicle. (A) Illustration of the rice panicle structure. The area indicated by the dashed box corresponds to the area within the dashed box in (B). (B) Illustration of lateral water flow, sucrose solution flow and sucrose loading/unloading. The leaf, two spikelets and two junctions are highlighted. Detailed explanations are given in the Materials and Methods.

daughter tubes have the same size. In contrast, when σ is close to 1, the main daughter tube has almost the same radius as its mother tube, whereas the subdaughter tube is extremely thin.

In both models, flow of solution in sieve tubes was assumed to obey the Hagen–Poiseuille law, by which flux is proportional to the fourth power of the tube radius [Equation (3) in the Materials and Methods]. It follows that the radius allocation rule greatly influences the efficiency of sucrose transport in the aorta model. To predict the growth of each grain in the panicle, we modeled the dynamics of sucrose concentrations at terminal points (the leaf and spikelets) and branching points. The amount of sucrose accumulating in each grain is proportional to the grain dry mass and is henceforth referred to as the grain size. We calculated grain growth in each spikelet based on the sucrose concentration dynamics. In addition, a plant's grain yield was measured as an index defined as the sum of normalized weights of all grains of size greater than a threshold w^* determined by a market-related factor [Equation (11) in the Materials and Methods]. A sufficiently nourished plant with M grains, therefore, attains a grain yield close to the potentially maximum value M.

Simulating grain growth in a Koshihikari panicle structure

We first performed numerical simulations of the model using a scanned panicle structure of the Koshihikari cultivar (see 'Parameter estimation' in the Materials and Methods) and compared the results for the pipe and aorta models. The actual panicle structure used in this study developed branches of up to second order (secondary branches) (**Supplementary Fig. S1**).

In the pipe model, grain yield started increasing approximately 20 d after heading (**Fig. 3A**). Because the radius of each sieve tube is the same in the pipe model, a shorter distance between the spikelet and source (the leaf) resulted in faster grain growth, although it is not pronounced in **Fig. 3A**.

Grain growth pattern predicted by the aorta model depended strongly on the magnitude of the allocation parameter σ. When half of the potential radius for two daughter tubes was assigned to each of the two daughter tubes at each branching point ($\sigma = 0.5$), basal grains on secondary branches grew sufficiently large, whereas the apical grain on each primary branch did not mature properly, resulting in a low yield (**Fig. 3B**). This is because the main sieve tube becomes thinner and thinner after branching, reducing the efficiency of sucrose transport to the tips of the branches. As σ increased, sucrose was transported to both the apical and bottom grains almost evenly, resulting in a homogeneous growth pattern regardless of grain position (**Fig. 3C**). When the allocation of radius to the main branch was close to the maximum ($\sigma = 0{\cdot}99$), the apical grains matured to a sufficiently large size, but the basal grain size became smaller (**Fig. 3D**) owing to sufficient (limited) sucrose transport via the primary (higher order) branches. Although grain yield started increasing rapidly, approximately 15 d after heading owing to the earlier maturation of apical grains, the increase slowed because of limited sucrose supply to basal grains on secondary branches.

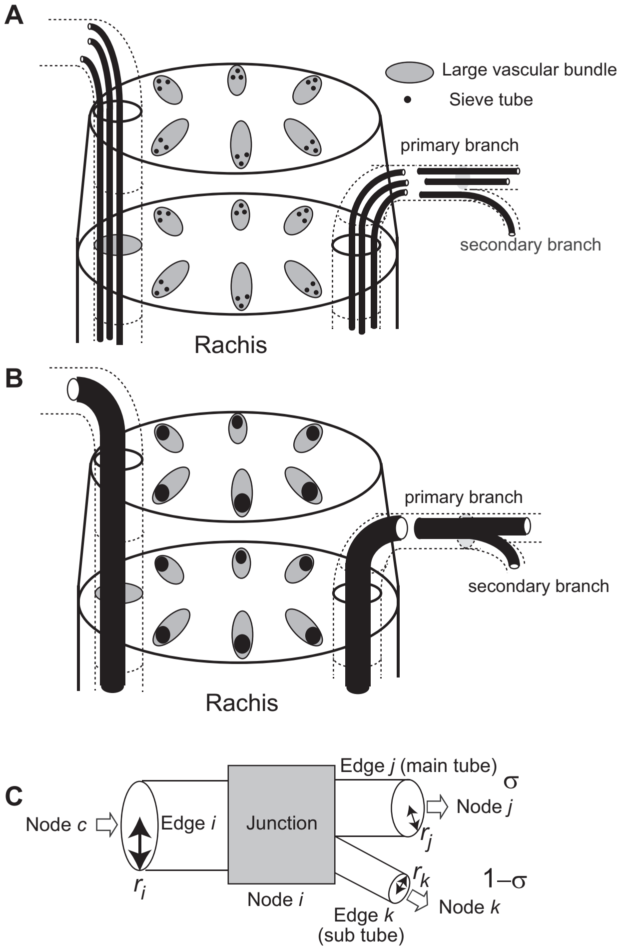

Fig. 2 Two models for the phloem network and radius allocation rule. (A) The pipe model. One of the large vascular bundles highlighted as white is allocated to a primary branch. A large vascular bundle contains multiple sieve tubes, each of which is allocated to a single spikelet. (B) The aorta model. Multiple sieve tubes in the large vascular bundle are approximated as a single large tube. At each branching point of primary or higher order branches, the tube bifurcates into two daughter tubes. (C) Relationship between three types of sieve tube radii in a primary or higher order branch of the aorta model. Edge *i* is the mother tube, and edges *j* and *k* are the main and sub-daughter tubes, respectively. Radii of these tubes follow $r_i^{\kappa} = r_j^{\kappa} + r_k^{\kappa}$ ($\kappa = 3$ in the present analyses).

These results clearly indicate the existence of competition among grains for sucrose [a simple distance-dependent competition for the pipe model; a complex position-dependent (distance- and σ-dependent) competition for the aorta model]. Thus, maximization of the efficiency of sucrose transport on a global panicle network scale is crucial to increase grain yield. Next, we investigated the phloem network structure that maximizes grain yield.

Optimal branching rule maximizing grain yield

In the aorta model, comparison of grain yield between different values of the allocation parameter σ showed that there is a unique σ that maximizes grain yield (the 'optimal σ' in Fig. 4A). With the optimal σ, which was $\sigma = 0.84$ for the panicle networks used in the analyses (see Table 1), grains at different positions in the panicle grew almost uniformly (Fig. 3C). In contrast, when σ is smaller or larger than the optimal, the between-grain variance in grain size was larger (Fig. 3B, D). These results indicate that for yield maximization it is preferable to have an allocation parameter that allows uniform sucrose transport to different grains in the network. In addition, we confirmed that an increase or a slight decrease in sucrose-producing capacity of the leaf hardly changed the optimal value for σ. It follows that there is an optimal value for the allocation parameter unique to a phloem network structure as long as sucrose supply is sufficient.

The grain yield predicted by the pipe model was lower than that generated by the aorta model with optimal σ (Fig. 4A). This is because the flow of phloem sap obeys Hagen–Poiseuille's law [Equation (3) in the Materials and Methods], under which one large tube (appearing in the aorta model; Fig. 2B) provides better translocation efficiency than multiple small tubes in the pipe model (Fig. 2A).

Comparison of grain growth between simulated and observed data

To investigate whether the simulated grain growth generates realistic behavior, we compared simulated and observed data. We obtained the position-dependent grain weight in the Hitomebore cultivar at the final stage of grain maturation ($n = 609$ from five panicles) and extracted two conditions that characterize real grain growth.

The first condition is the position-dependent difference in grain weight in a primary branch. Among the grains generated on a primary branch, the weight of the most basal grain was almost always greater than that of the grain at the tip (48 of 49 sampled pairs; paired *t*-test, $P < 0.001$; Fig. 4B). We named this feature condition I. The second condition is the difference in grain weight between primary and secondary branches. The average weight of grains on primary branches is greater than that of grains on secondary branches (one-way analysis of variance, $n_1 = 290$, $n_2 = 319$, $P < 0.001$; Fig. 4B). We named this trend condition II. These two conditions have been previously reported in other *japonica* cultivars (Nagato 1941, Hoshikawa et al. 1984).

We investigated when these two conditions are satisfied in simulated rice panicles. In the aorta model, condition I was satisfied when σ was ≥ 0.73 (median values are used throughout this paragraph, $n = 3$), whereas condition II was met when σ was ≤ 0.92. This result indicates that the feasible range of σ that captures realistic grain growth is between 0.73 and 0.92 (Table 1; Fig. 4A). Interestingly, optimal σ that maximizes grain yield was located within the feasible range (Table 1; Fig. 4A), suggesting that the position-dependent grain growth observed in common cultivars is a consequence of yield-maximizing selection. Grain growth data generated by the pipe model satisfied condition I but did not satisfy condition II, i.e. our pipe model does not capture realistic grain growth. Thus, we henceforth focus on the analysis of the aorta model. Note that the two conditions could be satisfied if we relax the assumptions of the pipe model (e.g. allowing tapering).

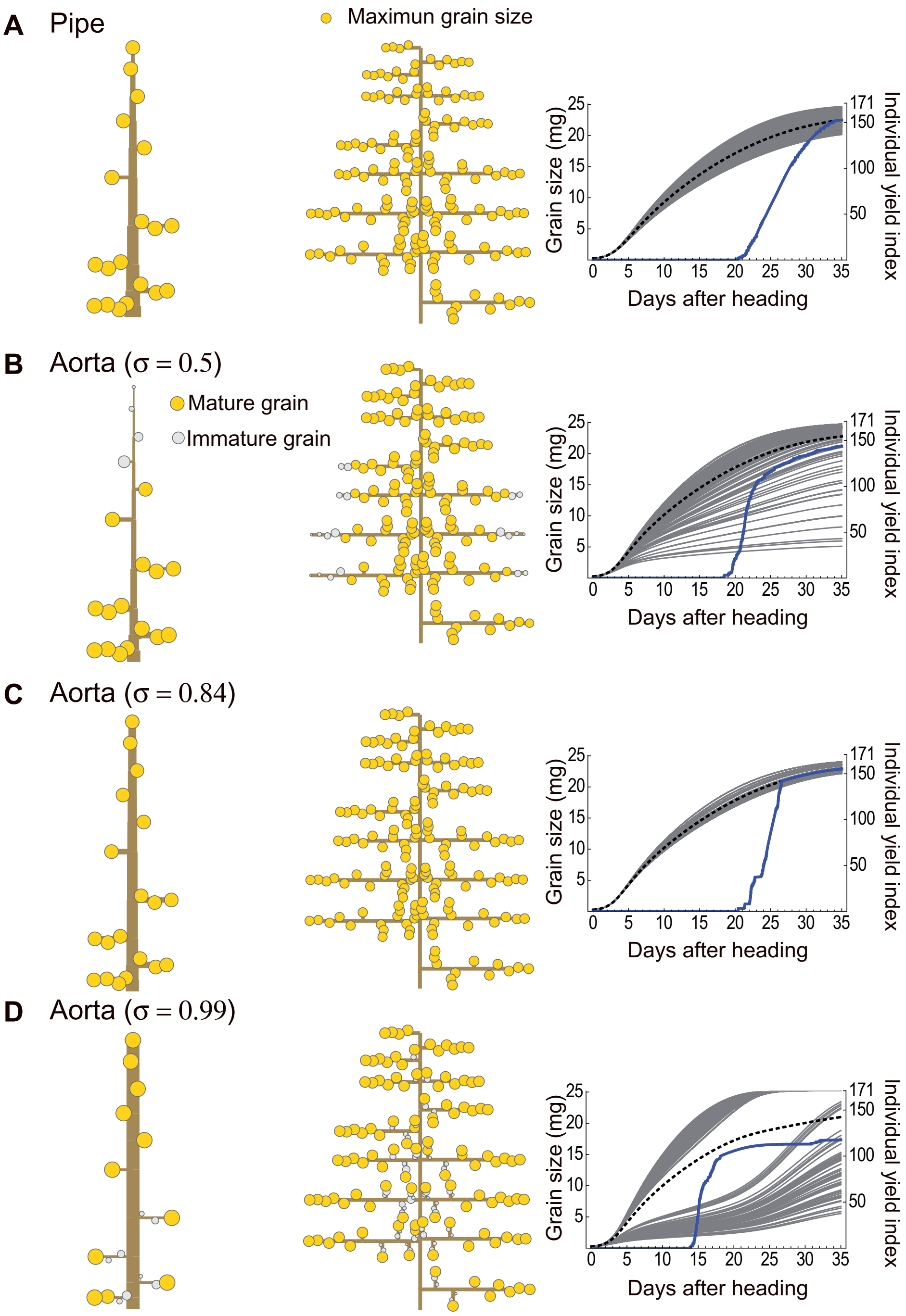

Fig. 3 Comparison of simulated grain growth between the pipe and aorta models. (A) The pipe model. (B) The aorta model with allocation parameter σ = 0.5. (C) The aorta model with σ = 0.84. (D) The aorta model with σ = 0.99· Left panels represent the thickness of sieve tubes and final grain sizes of the second bottom primary branch. The yellow and gray circles represent mature and immature grains, respectively. Center panels represent the final grain sizes of the panicle. Right panels indicate the time course of growth of each grain (thin lines), average grain growth (dashed lines) and individual grain yield (blue lines).

Finding an optimal grain arrangement under the same grain number

Recent advances in molecular and genetic studies have allowed the modification of panicle structure to increase grain yield. Essentially, the modification of panicle structure results in a change in both grain number and grain arrangement. To design a panicle structure that realizes efficient sucrose transport and a high grain yield, we separately assessed the effect of grain number and grain arrangement on grain yield using a mathematical model. We first investigated the optimal panicle branching network under a fixed number of grains.

Following Matsuba (1991), we created three hypothetical primary branch networks by fixing the number of grains and

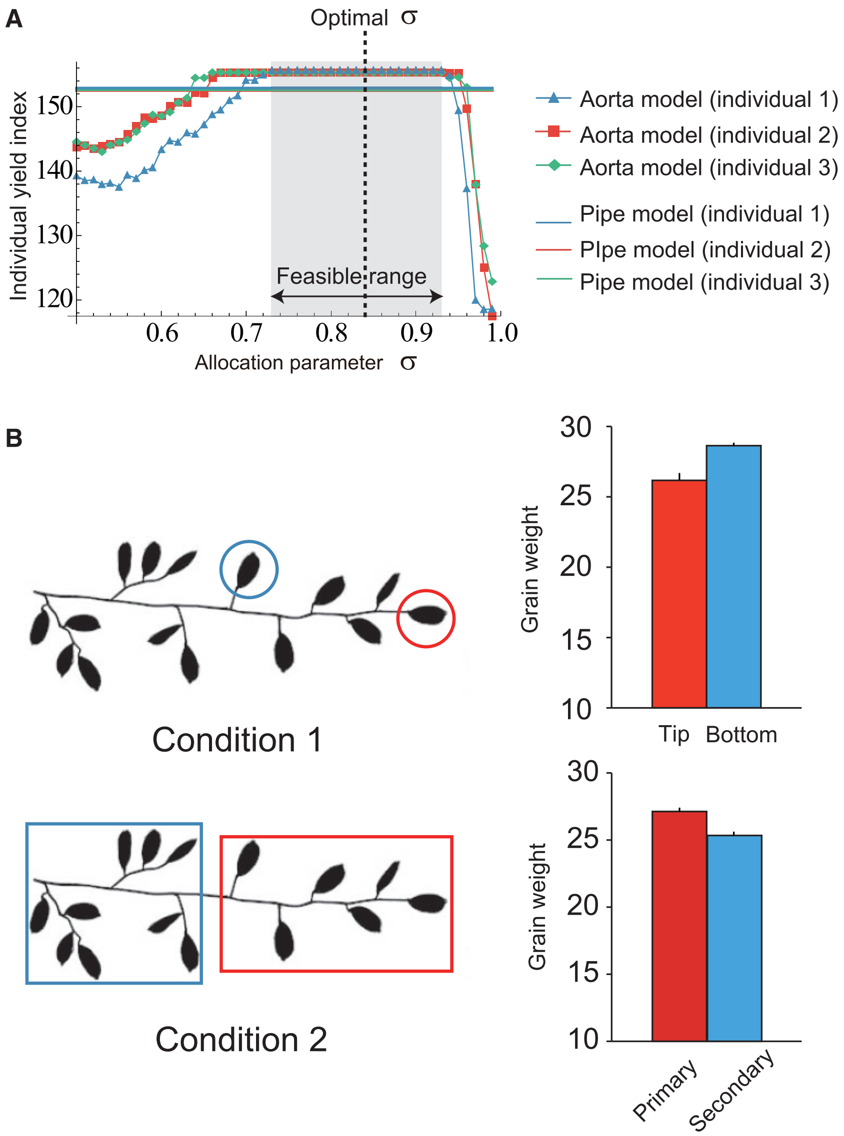

Fig. 4 Finding optimal and feasible values for allocation parameter σ. (A) Comparison of individual grain yield between different models and different values of σ. Panicle networks obtained from three different individuals of the Koshihikari cultivar were used. For the aorta model, the σ maximizing grain yield was 0.84 and is shown as a dashed line. The gray square represents the feasible range of σ that satisfies two conditions explained in (B) $(0.73 < \sigma < 0.92)$. (B) Two conditions characterized from the grain growth data of the Hitomebore cultivar. Condition I: among the grains generated on a primary branch, the weight of the most basal grain (blue) is almost always greater than that of a grain at the tip [red; paired *t*-test, $n_{(pair)} = 49$, $P < 0.001$]. Condition II: the average weight of grains on primary branches (red) is greater than that of grains generated on secondary branches (blue; one-way analysis of variance, $n_1 = 290$, $n_2 = 319$, $P < 0.001$). Error bars represent standard deviations.

Table 1 Feasible range and the optimal value of the allocation parameter for different panicle networks

ID	No. of grains (*M*)	Feasible σ	Optimal σ
1	171	0.73–0.92	0.84
2	171	0.73–0.91	0.85
3	180	0.75–0.92	0.84

We supposed that condition I holds for the shoot if condition I holds for more than half of its primary branches.

the total edge length (**Fig. 5B**; 'Designing hypothetical panicle networks' in the Materials and Methods; assuming the same grain number is necessary to study how network structure itself influences the grain yield) and compared the efficiency of sucrose transport and grain yield between these three different networks. Matsuba (1991) proposed the maximum branching model, which is a hypothetical panicle structure expanding all potential branches in a self-similar manner. The maximum branching model could be achieved without apical dominance, which is regulated by the balance of growth-promoting and inhibitory hormones in nascent juvenile organs (**Fig. 5A**), and is equivalent to a binary tree network. However, in rice panicles, the terminal inflorescence shows a strong apical dominance, inhibiting the development of axillary reproductive structures. Within the inflorescence, intergrain apical dominance regulates the growth of individual spikelets at the various nodes. Matsuba (1991) considered diverse panicle structures observed in real

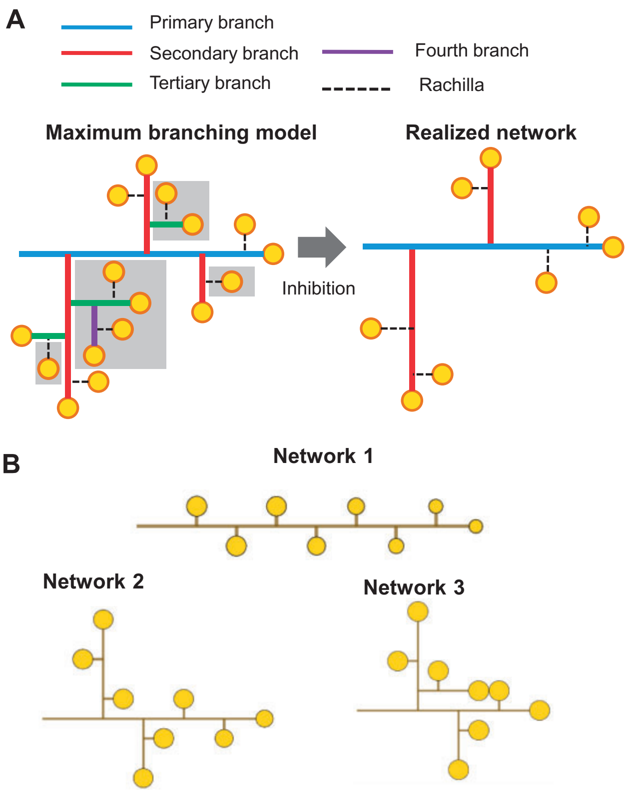

Fig. 5 Panicle networks and the maximum branching model. (A) Representation of the maximum branching model (left panel) and the realized grain network generated from the maximum branching model owing to branching inhibition by apical dominance (right panel). In this example, the maximum branching model develops up to the quaternary (fourth-order) branch, but only secondary branches emerge in the actual panicle network. We used the partial panicle structure including the single primary branch. Squares indicate branches that will be lost owing to branching inhibition. Each pedicel ends with a spikelet at the terminal end. (B) Three hypothetical grain networks. Network 1: branching inhibition is strong, and no secondary or higher order branches emerge. Network 2: branching inhibition is intermediate, and two secondary branches appear. Network 3: the maximum branching model developing up to tertiary branches.

rice cultivars as a consequence of apical dominance occurring at different timings and intensities during panicle development, and generated varieties of hypothetical panicle networks (**Fig. 5A**). Although the maximum branching model has never been realized in any rice cultivar, it is useful for understanding the basic panicle branching rules underlying the development of any cultivar and the branching inhibition rule specific to each cultivar.

In network 1, apical dominance is strong and there are no secondary or higher order branches; this suggests that all grains are attached to the primary branch (**Fig. 5B**). In network 2, apical dominance is intermediate, and grains are attached to both primary and secondary branches (**Fig. 5B**). Among the 63 potential networks that have ≥ 8 grains on secondary branches, we chose network 2 because it had secondary branches at the basal part of the primary branch, an arrangement that resembles the panicle structure of common cultivars (**Supplementary Fig. S1**). Network 3 has a tertiary branch at the basal part of the bottom secondary branch. Note that network 3 is equivalent to the maximum branching model with little apical dominance. Most primary branches of common rice cultivars fall into the same group as networks 1 and 2, given that they develop up to secondary branches. However, we rarely see primary branches similar to those of network 3 (those with one or more tertiary branches), and most are observed in mutant cultivars with an increased grain number (Kobayashi et al. 2010, Yoshida et al. 2013).

The grain arrangement that maximized grain yield varied depending on the allocation parameter σ. Within the feasible range of σ, network 1 or 2, both of which are frequently observed in common rice cultivars, as mentioned above, was the optimal network (**Fig. 6A**). When a value not exceeding 0.81 was assigned to σ, network 2, which has up to secondary branches, attained the highest yield. When σ was >0.81, sieve tubes in the secondary branches of network 2 were too narrow to transport sufficient sucrose, and the optimal network accordingly shifted from network 2 to network 1 (**Fig. 6A–C**). Network 3 was always less efficient than either or both of networks 1 and 2 within the feasible range (**Fig. 6A**), because a larger ratio of the sieve tube radius to the main tube radius at lower order branches narrowed the sieve tubes at higher order branches (especially at the tertiary branch), resulting in highly inefficient sucrose transport and poor grain growth (**Fig. 6D**). These results show that the efficiency of sucrose transport is affected by grain arrangement and that there is a strong transport limitation in network 3.

We next investigated how the capacity of the source influences optimal grain arrangement by increasing the net sucrose production rate represented by the difference between γ_0 and h_0 in Equation (7) (see the Materials and Methods). As shown in **Fig. 6A–D**, predicted grain yield did not reach the maximum possible yield of 8 regardless of the network structure, implying the effect of source limitation. When the sucrose production rate was doubled, grain yield predicted by all the networks was almost the same as the maximum possible yield even when σ was relatively small (**Fig. 6E**), suggesting no source limitation. Even if there was no source limitation, the best network was the same; network 2 was best when σ was ≤ 0.81, whereas network 1 was best when σ was >0.81 within the feasible range of σ (**Fig. 6E**). This result indicates that the optimal grain arrangement and the source capacity affect individual plant yield mutually independently. In addition, a plant with network 2 or network 3, especially the latter, did not attain a sufficient grain yield when a large value was assigned to σ. It follows that grains of a plant with an inappropriate network cannot fully mature, owing to transport limitation even without source limitation.

Finding the optimal grain number

We investigated how an increase in grain number contributes to grain yield using the simplest primary branch networks with no higher order branches (network 1 in **Fig. 5B**). Starting from a single grain network, grain yield increased with grain number,

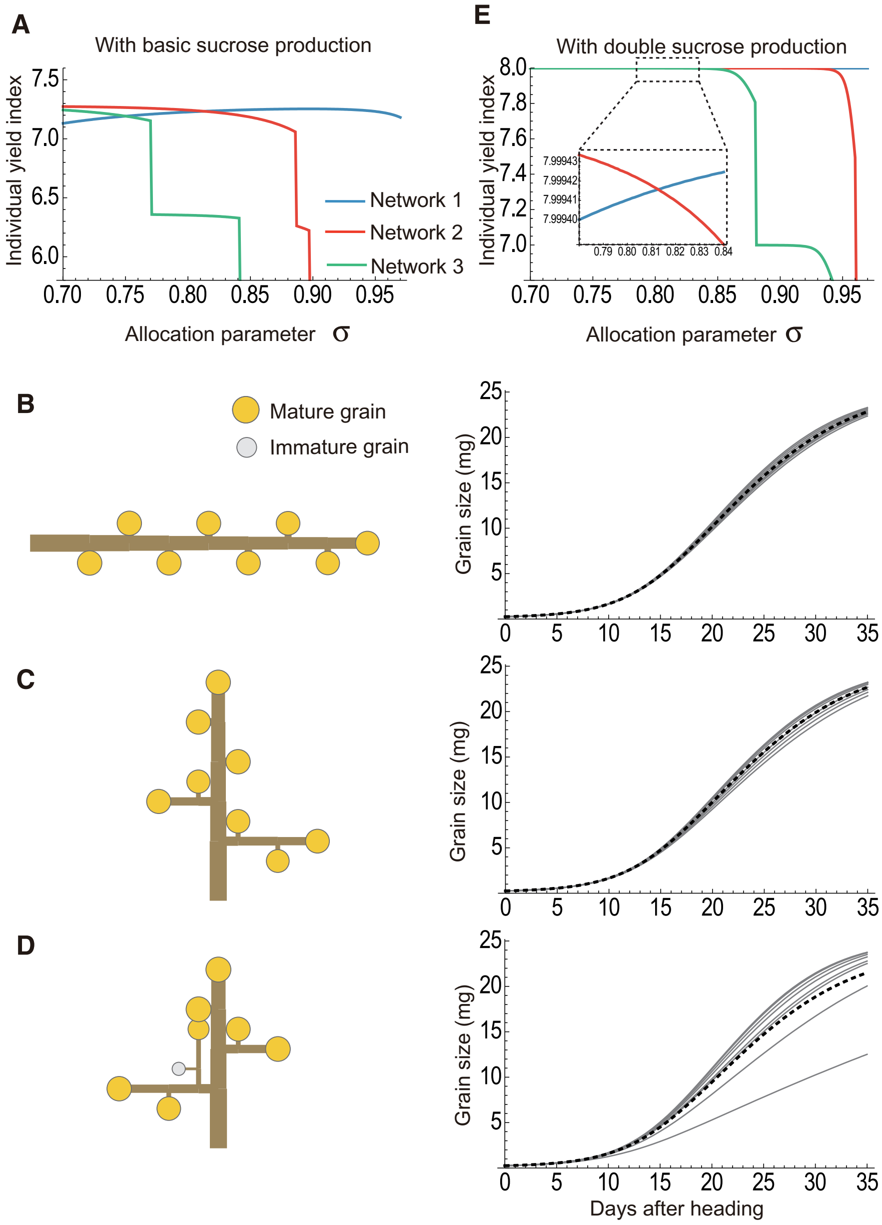

Fig. 6 Comparison of individual grain yield and grain growth between different grain networks. (A) Network-dependent grain yield as a function of allocation parameter σ. Optimal values for the allocation parameter σ were 0·90, 0·67 and 0.54 for network 1, 2 and 3, respectively. (B–D) Position-dependent grain size at the final growing stage, and the time course of growth of each grain predicted in the three different grain networks. Dashed lines represent the average ($\sigma = 0.84$). Here we used the partial panicle structure, namely one primary branch and zero or two accompanying secondary branches, for our analysis; however, parameters have been estimated using the whole panicle including 14 primary and multiple secondary branches (Materials and Methods). Because the total grain number considered here is approximately 20 times smaller than that of a whole panicle, an excessive amount of sucrose is allocated to each grain, resulting in unrealistically rapid growth when we use the parameter values summarized in **Table 1**. We accordingly adjusted the values of the sucrose synthesis rate (γ_0) and respiration rate (h_0) to 14 times smaller than the original values, given that common *japonica* cultivars develop approximately 14 primary branches. We also adjusted the value of initial sucrose concentration at node 0 [$s_0(0)$] to four times smaller than the original to reduce the deviation between the model and the data in the time course of grain growth. The new parameter set we obtained is $\{\gamma_0, h_0, s_0(0)\} = \{1.75\times10^{-9}, 8.20\times10^{-10}, 143.45\}$. (E) Network-dependent grain yield as a function of allocation parameter σ when the net sucrose production rate of the leaf (i.e. $\gamma_0 - h_0$) is doubled. Optimal values for the allocation parameter σ were 0·90, 0·67 and 0.53 for network 1, 2, and 3, respectively, indicating that the optimal σ hardly changes with increasing sucrose production.

as expected. However, when grain number exceeded 9, a further increase resulted in a drastic decrease in grain yield (**Fig. 7A**). A 16-grain network even attained no yield. This is because all grains in the 16-grain network cannot reach the grain size necessary for the market, owing to sucrose competition among grains (**Fig. 7A**). The amount of sucrose transported to immature grains was simply wasted, as they had no market value.

Table 2 Best-fit values for the sucrose unloading rate (α) with different panicle structures

ID	σ				
	0.5	**0.6**	**0.7**	**0.8**	**0.9**
1	9.3×10^{-9}	9.1×10^{-9}	9.0×10^{-9}	8.9×10^{-9}	8.9×10^{-9}
2	9.3×10^{-9}	9.0×10^{-9}	8.9×10^{-9}	8.9×10^{-9}	8.9×10^{-9}
3	1.2×10^{-8}	1.1×10^{-8}	1.1×10^{-8}	1.1×10^{-8}	1.1×10^{-8}

When the sucrose production rate was doubled, increase of grain number contributed more to grain yield. Grain yield continuously increased up to 16 grains (**Fig. 7B**). However, as in **Fig. 7A**, a further increase in grain number did not contribute to increasing grain yield. The grain number that maximized the grain yield increased with the sucrose production rate (**Fig. 7C**), suggesting the need for a balance between the supply and consumption of sucrose to realize high grain yield. In the different panicle networks that developed higher order branches, we also observed that an excessive increase in grain number reduced grain yield (**Supplementary Fig. S2**).

Discussion

Designing optimal grain number and arrangement for high grain yield is a complex problem because grain yield is intimately intertwined with multiple factors, such as source, sink and translocation capacities. Our model helps in finding numerical solutions for optimal panicle structure under various source and sink capacities.

The model predicted that the optimal structure for high yield corresponds to a simple grain arrangement on a primary branch with no higher order branching (network 1; **Fig. 5B**) or with only secondary branches (network 2; **Figs. 5B**, 6A). In the optimal panicle structure, sucrose is efficiently transported to each grain and all grains develop and mature equally (**Fig. 6B**). In contrast, a panicle structure that develops tertiary branches (network 3; **Fig. 5B**) suffers from translocation limitation, in which a limited amount of sucrose is transported to grains attached on tertiary or secondary branches, resulting in poor maturation (**Fig. 6D**). These results imply that to increase grain yield, increasing the numbers of grains on primary or secondary branches would be preferable rather than developing tertiary branches. Our theoretical findings are consistent with the panicle structure of modern cultivars; networks 1 and 2 are frequently found in upper and lower parts of panicles, respectively (e.g. in the Koshihikari cultivar in **Supplementary Fig. S1**), whereas network 3 is rarely observed except in mutants (Kobayashi et al. 2010, Yoshida et al. 2013).

In the equation of Hagen–Poiseuille flow [Equation (3) in the Materials and Methods], the volume flow rate depends on the fourth power of the sieve tube radius, i.e. doubling the radius of the tube will result in a 16-fold increase in the volume flow rate. Regardless of its importance, little is known about how sieve tube radius is distributed in rice panicles and how a single tube bifurcates at each junction of primary or higher order branches. In this study, we used two very different models, pipe and aorta models, to determine the unknown structure of sieve tubes. By comparing the predicted and observed grain growth patterns, we demonstrated that the

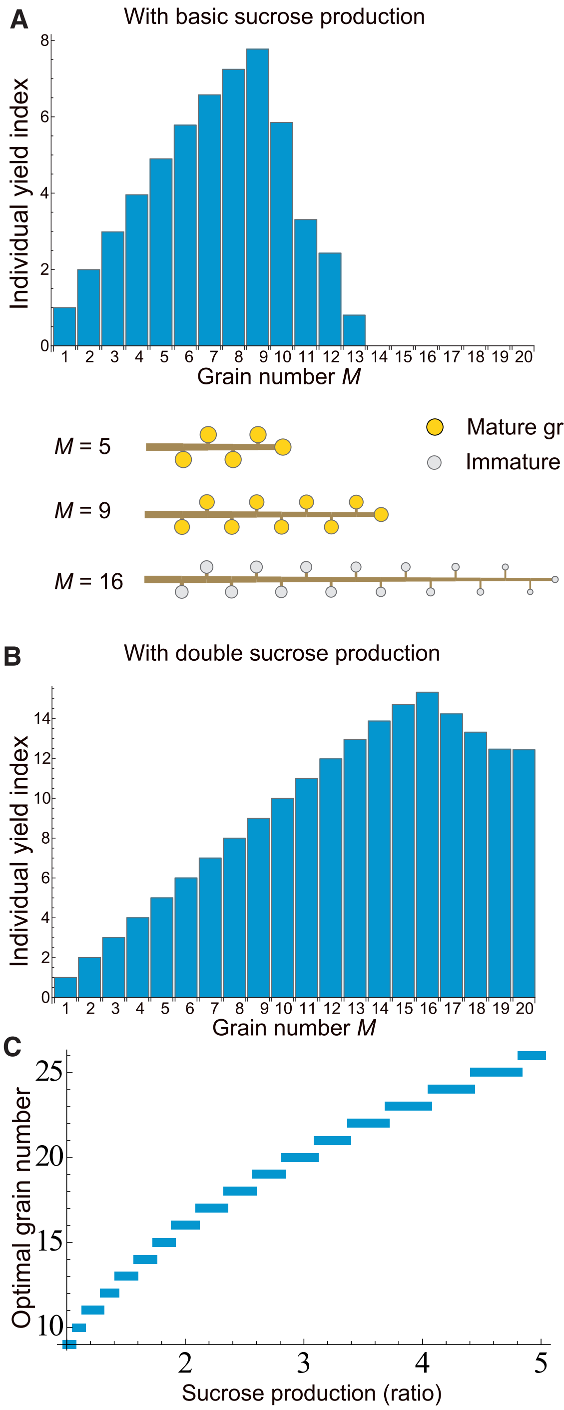

Fig. 7 Relationship between grain number and individual grain yield in network 1. (A) The initial sucrose synthesis rate (γ_0), respiration rate (h_0) and sucrose concentration at the leaf [$s_0(0)$] are 1.75×10^{-9}, 8.20×10^{-10} and 143.45, respectively. (B) The net sucrose production rate of the leaf ($\gamma_0 - h_0$) is doubled. (C) Relationship between sucrose synthesis rate and the grain number that maximizes grain yield. Increasing leaf aging parameter (b) or sucrose loading rate (a) yielded almost the same result (data not shown).

Table 3 Parameters and variables used in the present model

		Definition	Unit	Used value	Measurement	Cultivar or species
Parameters	A_{leaf}	Leaf blade area	m^2	1.34×10^{-2}	Maruyama and Tajima (1988)	Japonica, improved
	a	Proportion of sucrose loaded into collection phloem		0·4		
	b	Potential leaf longevity	s	3014000 (35 d)	Hidema et al. (1991)	Sasanishiki
	g_0	Gross photosynthetic rate of the leaf at time zero	$mol\,s^{-1}$	$A_{leaf} \times 2.36 \times 10^{-6}$	Hidema et al. (1991); Hirai et al. (2003)	Indica and Japonica
	h_0	Respiration rate of the leaf at time zero	$mol\,s^{-1}$	$g \times 0.36$	Hirai et al. (2003)	Indica and Japonica
	l_i	Sieve tube length	m	$l_{-1} = 0.3$ Values obtained from 2D-scanner data for $i \neq -1$	This study	Hitomebore Koshihikari
	L	The number of large vascular bundle in a panicle				
	m	Per area membrane permeability at Node-*i*	$Pa^{-1} m s^{-1}$	5.0×10^{-14}	Reviewed in Thompson and Holbrook (2003a)	Trees
	m_i	Membrane permeability at Node-*i*	$Pa^{-1} m^3 s{-}^{1}$	$m \times 10^{-4a}$ for $i = 0$ $m \times 10^{-5a}$ for $i \in \{1,..., M\}$		
	M	The number of spikelets (grains) in a panicle				
	N	The number of junctions in a panicle				
	r_i	Edge (sieve tube) radius	m	$r_{aortaL} = 8.0 \times 10^{-6}$ Calculated for the other points	Nakamura et al. (unpublished)	Hitomebore
	R	Gas constant	$Pa\ m^3 K^{-1} mol^{-1}$	8.31	CODATA	
	T	Air temperature	K	298.15 (25°C)		
	v_i	Volume of Node-*i*	m^3	$1{\cdot}34 \times 10^{-6}$ for $i = 0$ $\pi r_i^2 l_i$ for $i \neq 0$		
	w^*	Threshold grain size for sale	mol	$20 \times 10^{-3} \times W_2/W_3$	This study	Hitomebore
	W	Maximum sucrose amount a grain can accumulate	mol	$W_1 W_2/W_3$		
	W_1	Maximum weight of brown rice	g	25.21×10^{-3}	This study	Hitomebore
	W_2	Proportion of carbohydrate to brown rice weight		0.738	MEXT, Japan (2005)	
	W_3	Molecular weight of sucrose	$mol^{-1} g$	342·3	CODATA	
	α	Sucrose unloading rate	$m^3 mol^{-1} s^{-1}$	1×10^{-6}	This study[b]	
	γ_0	Average sucrose synthetic rate of the leaf at time zero	$mol\,s^{-1}$	$g_0 \times 7/9$ ($g_0 \times 14/24 \times 100/75$)	Cock and Yoshida (1972); Hirai et al. (2003)	Indica and Japonica
	η	Solution viscosity[c]	Pa s	8.9×10^{-4}	CODATA	
	κ	Exponent for the power-law on branching process		3		
	σ	Proportion of sieve tube radius allocated to main daughter tube		0.5–0.99	This study[b]	
Variables	$p_i(t)$	Turgor pressure at Node-*i*	Pa			
	$s_i(t)$	Sucrose concentration at Node-i	$mol\,m^{-3}$	$s_i(0) = 0$ for $i \neq 0$ $s_0(0) = 573{\cdot}8$	Hayashi and Chino (1990)	Kantou
	$w_i(t)$	Sucrose amount of Grain-*i* at time *t*	mol	$w_i(0) = W \times 1/100$		
	$Y(t)$	Yield at time *t*	mol			

Molar amount was counted as sucrose (C_{12}).

[a] 10^{-4} and 10^{-5} are the values assigned to membrane surface areas of the leaf and each spikelet, respectively. We speculated that the former would greater than the latter because the leaf in our model corresponds to a set of leaves each of which contains multiple veins.

[b] The values were not measured but estimated by model fitting.

[c] The value for pure water viscosity at 25°C was used as a surrogate for the actual viscosity function depending on sucrose concentration and temperature.

aorta model is more appropriate than the pipe model. This result suggests that the bifurcation of a single sieve tube is likely to occur in real rice panicles. Our prediction needs to be tested by studying the phloem anatomy, but currently few data are available (e.g. Nakamura and Hoshikawa 1985). Using new imaging techniques would be useful to explore the complex structure of the sieve tube network in rice panicles (Truernit 2014). Phloem imaging would also help to measure directly the allocation parameter, the most important parameter determining radius distribution in the aorta model. If the directly measured allocation parameter for some cultivars is smaller than the indirect estimate in this study, the panicle structure with tertiary or higher order branches might be selected as the optimal structure for those cultivars to attain high yield (an increased yield is expected in the network 3 when σ is small; **Fig. 6A**). Identifying genes or QTLs regulating sieve tube number or its radius allocation rule would contribute to marked enhancement in plant yield, as demonstrated by the *HI1* allele of *APO1* (Terao et al. 2010) or *SPIKE* (Fujita et al. 2013).

We confirmed that our conclusion (networks 1 and 2 are superior to network 3 with respect to grain yield) was robust even when we increased source capacity. This result indicates that translocation limitation, in the form of inefficient delivery of assimilated carbon from source leaves to panicle sinks, prevails regardless of source capacity. The effects of a limited number or size of sieve tubes (Terao et al. 2010) and activity of phloem sucrose loading and unloading (Braun et al. 2014) have also been proposed as factors regulating translocation limitation. However, how the arrangement of grain influences the transport efficiency of sucrose and how it determines grain yield have not been examined quantitatively. Our study emphasized the unexplored effect of grain arrangement in a panicle on grain yield, and showed that strong translocation limitation can occur in panicles with many higher order branches even in the absence of sink and source limitations (**Fig. 6A**, E). Our model will also help to estimate the maximum sink capacity (maximum number of grains) allowed under various source and translocation capacities (**Fig. 7**; **Supplementary Fig. S2**).

To improve the performance of the model, several extensions are needed. First, the magnitude of sucrose unloading ability of each sink [α in Equation (10) in the Materials and Methods] can be position dependent, as suggested by Yang et al. (2006). For this extension, we need data describing sucrose unloading ability in grains located at each different position in a panicle. Secondly, we can incorporate the differences in fertilization timings between spikelets in the same panicle. For this purpose, careful monitoring of position-dependent timing of flowering and fertilization in each spikelet, as performed by Nagato (1941) and Hoshikawa (1989), is necessary. Alternatively, the panicle developmental process can be modeled by considering hormonal networks involved in the control of shoot branching (Domagalska and Leyser 2011) to explain why the timing of flowering and fertilization differ between grain positions.

In the present study, we theoretically demonstrated that panicle structure plays a key role in determining grain yield. From the evolutionary point of view, our study raises a new question: how and why does diversity in grain arrangements emerge? Even within the same rice species, different varieties show different grain arrangements. Differences in panicle structures in rice are pronounced when domesticated cultivars are compared with wild types (Sweeney and McCouch 2007). The same differences have been identified among monocot crop species (Bonnett 1966). The diversity of panicle structure can be an outcome of natural or artificial selection acting to optimize the reproductive success of wild rice itself or increase yield for humans. Detailed comparative studies focusing on the difference between panicle structures of wild and domesticated lines will not only reveal the unrecorded history of artificial selection, but will also shed light on the future development of improved (high-yielding) cultivars.

Materials and Methods

Graph illustration of panicle structure

We consider a phloem structure on a graph composed of edges corresponding to sieve tubes and three kinds of nodes: leaf (node 0), spikelet (node 1 to node M) and junctions [node ($M + 1$) to node ($M + N$); **Fig. 1B**]. Each edge is considered as a perfect cylinder with radius r_i (m) and length l_i (m) ($i \in \{1, \ldots, M + N\}$). The number of primary branches is denoted as L. In *japonica* cultivars, the total number of large vascular bundles in a panicle is also L.

The leaf, here denoted as node 0, includes multiple sieve tubes in which assimilated sucrose is loaded into collection phloem. Each branch ends with a spikelet that is assumed to comprise a grain and a sieve tube, where unloading of sucrose and growth of the grain occur. Each junction corresponds to the bifurcation point of a sieve tube.

The pipe and aorta models

The assumptions of our pipe model are as follows: the ith bundle contains n_i sieve tubes. At the bottom of the panicle in the rachis, n_i sieve tubes included in the focal vascular bundle are assigned to the ith primary branch (**Fig. 2A**). Each sieve tube in the ith primary branch is allocated to one spikelet. Thus the number of spikelets in the ith primary branch equals n_i and the total number of spikelets in the whole panicle, denoted as M, is calculated as the sum of sieve tube numbers contained in each large vascular bundle; $M = \Sigma_{(i)} n_i$. All sieve tubes have the same radius, r_{pipe}. Given that A_0 is the sum of the cross-sectional areas of all sieve tubes, $r_{\mathrm{pipe}} = [A_0/(\pi M)]^{1/2}$.

In our aorta model, there are L large and independent sieve tubes at the bottom of the panicle (**Fig. 2B**). The radius of each large sieve tube is the same and is denoted by r_{aortaL}. Using the same value as in the pipe model, A_0, as the sum of cross-sectional areas of all large sieve tubes, r_{aortaL} is calculated as $[A_0/(\pi L)]^{1/2}$.

Bifurcation of a tube in the aorta model

For a phloem network designed as an aorta model, the relationship between the radii of mother and daughter tubes at each branching point is of crucial importance for efficient sucrose transport. Radius allocation rules have been identified in animal (LaBarbera 1990) and plant vascular systems (West et al. 1999, McCulloh et al. 2003). In an optimally designed vascular system that minimizes energy expenditure, at any branching point the κth power of the radius of the mother tube will equal the sum of the κth powers of the radii of the daughter tubes (Durand 2006):

$$r_i^{\kappa} = r_j^{\kappa} + r_k^{\kappa}, \qquad (1)$$

where r_i , r_j and r_k represent the radii of the mother tube, the main daughter tube and the subdaughter tube, respectively (**Fig. 2C**). When $\kappa = 2$, Equation (1) corresponds to da Vinci's law by which cross-sectional area is conserved after branching, whereas when $\kappa = 3$, it corresponds to Murray's law (Murray 1926). Experimental data on trees suggest the validity of Murray's law for vessel (xylem) branching (McCulloh et al. 2003), but less information is available on rice. In this study, we adopted Murray's law for two reasons: (i) the qualitative behavior of the aorta model was not different between the two laws; and (ii) Murray's law always resulted in higher grain yield than da Vinci's law.

In the aorta model, another rule that specifies the assignment of radius to different daughter tubes is necessary for determining the relative radius of each daughter tube after branching. Using Equation (1), we developed the following σ rule (**Fig. 2C**):

$$r_j^{\kappa} = \sigma r_i^{\kappa}, \tag{2a}$$

$$r_k^{\kappa} = (1 - \sigma) r_i^{\kappa}. \tag{2b}$$

where σ ($1/2 < \sigma < 1$) is an allocation parameter. It means that the fraction σ of the κ power of the mother tube radius (r_i) is allocated to the main daughter tube, and the rest ($1 - \sigma$) is assigned to the subdaughter tube. Note that the radius of the main daughter tube increases with σ. This rule can be regarded as a natural extension of previous studies on plant development (Stein and Boyer 2006).

In the xylem systems of trees and vines, McCulloh et al. (2003) suggested that a combination of pipe and aorta models is most likely. However, currently little is known about the phloem system. We accordingly compared the results of the pipe and aorta models. In our comparison, we assumed that the sum of the cross-sectional areas of sieve tubes is the same (i.e. A_0) for the two models. In both models, flow of solution in sieve tubes was assumed to obey the Hagen–Poiseuille law in which flux is proportional to the fourth power of tube radius [see Equation (3)]. Thus, it follows that radius distribution greatly influences the efficiency of sucrose transport.

Sucrose solution flux in sieve tubes as Hagen–Poiseuille flow

To predict the growth of each grain in the panicle, we modelled the dynamics of sucrose concentration $s_i(t)$ (mol m^{-3}) at node i ($i \in \{0, \ldots, N + M\}$). The amount of sucrose accumulated in each grain was considered as the grain size.

Here we consider only one solute and use the terms solute and sucrose synonymously. Fluxes of sucrose solution and pure water are modeled based on the pressure–flow hypothesis in which solution flux between sink and source is determined by their hydrostatic pressure difference (Münch 1930). Let $J_j(t)$ (m^3 s^{-1}) [$-J_j(t)$] be the sucrose solution flow entering [leaving] node j from [for] the neighboring node located closer to the leaf, node i, at time t (**Figs. 1B**, **2C**). Because the effect of inertia is considered to be sufficiently small compared with fluid viscosity (Thompson 2006), we assume that sucrose solution flux J_j follows the Hagen–Poiseuille equation:

$$J_j(t) = \frac{\pi}{8\eta} \frac{r_j^4}{l_j} (p_i(t) - p_j(t)), \tag{3}$$

where η (Pa s) is the viscosity of the sap with sucrose concentration $s_j(t)$ at temperature T (Lang 1978), and $p_i(t)$ and $p_j(t)$ (Pa) represent the turgor pressure at nodes i and j, respectively. Note that this formalization assumes that tubes are free from obstructions such as sieve tube plates and that lateral water exchange is minimal. Effects of sieve tube plates vary among species (Thompson and Holbrook 2003b), but no data are available for rice. If the effects of sieve tube plates are included, the left-hand side of Equation (3) is multiplied by a certain coefficient, which becomes a position-independent constant under some assumptions [see Thompson and Holbrook (2003a) for more justification]. In that case, it can be mathematically shown that qualitative results obtained from the present model (in the form of optimal grain arrangement) remain unchanged. In addition, we expect that quantitative results (such as optimal grain number) would also hardly change as long as an estimated value for the parameter (α) is updated using the same observed data. Specifically, if we multiply the left-hand side of Equation (3) by β denoting the effect of sieve plate ($\beta < 1$), a value larger than the present value of 1×10^{-8} will be estimated for α to cancel out the effect of β on grain growth, and we will obtain grain growth curves highly similar to the present curves.

We assume that all parts other than the grains have no volume flexibility and thus that solution flow within the phloem is entirely due to the difference in turgor pressure between neighboring nodes.

Pure water flow between xylem and phloem

We assume that pure water enters/leaves the system at nodes where sucrose loading/unloading occurs, namely at the leaf and each spikelet, and thus that there is no lateral flow of pure water or solute at junctions and along edges. With this assumption, Kirchhoff's current law holds at each junction (**Figs. 1B**, **2C**):

$$J_i(t) = J_j(t) + J_k(t), \tag{4}$$

where J_i represents the flux entering node i, and J_j and J_k represent fluxes entering node j and node k (from node i), respectively, the positive sign convention being acropetal. Equation (4) indicates that the volume of sucrose solution entering the junction is equal to that leaving it.

At the leaf, sucrose solution outflow, $J_0(t)$, from the leaf must equal pure water inflow from the xylem. The direction of $J_0(t)$ depends on the difference between the osmotic pressure, which is calculated as $s_0(t)RT$ by the van't Hoff equation under the assumption of dilute solution, and the hydrostatic pressure at node 0, $p_0(t)$:

$$J_0(t) = m_0(s_0(t)RT - p_0(t)), \tag{5}$$

where R (Pa m^3 K^{-1} mol^{-1}) is the gas constant, T (K) is the absolute temperature, and m_0 (m^3 Pa^{-1} s^{-1}) is the product of membrane permeability and membrane surface area attaching to the companion cells at the leaf. Similarly, solution inflow into each spikelet must equal pure water outflow into the xylem as follows:

$$J_k(t) = m_k(p_k(t) - s_k(t)RT), \tag{6}$$

where m_k (m^3 Pa^{-1} s^{-1}) is the product of membrane permeability and membrane surface area at node k ($k \in \{1, \ldots, M\}$; **Fig. 1B**).

By solving a set of simultaneous linear equations for $p_i(t)$ [Equations (3)–(6), $i \in \{0, \ldots, M + N\}$], we obtain an algebraic form for $p_i(t)$ that depends only on $s_i(t)$. Then $J_i(t)$ is calculated by substituting $p_i(t)$ into Equation (3). Note that $J_i(t)$ can take negative values.

In every numerical simulation of the present study, we approximately regarded sap viscosity η as constant throughout the whole simulation in spite of time- and position-dependent sucrose concentration. We confirmed that this approximation did not greatly affect the model outcomes by comparing the outcomes using constant viscosity with the outcome using a proper viscosity function dependent on sucrose concentration (Lang 1978). The approximation greatly shortened the computational time required for solving the linear equations. It is important to note that we found translocation limitation in some rice panicles even with the least value for constant viscosity (i.e. viscosity of pure water), with which sap flux was maximized. The translocation limitation will be more severe with the proper viscosity function because total sap flux must be smaller than the case of pure water.

Sucrose concentration dynamics and grain growth

Here we explain the dynamics of sucrose concentration at the three kinds of nodes (leaf, junction and spikelet). Sucrose concentration dynamics at the leaf (node 0) are given as follows:

$$\frac{ds_0(t)}{dt} = \frac{1}{v_0} \left\{ a\left(\gamma_0 - h_0\right)\left[1 - \frac{t}{b}\right]_+ + \sum_{i \in \mathbf{D}} (s_i(t)[-J_i(t)]_+) - s_0(t) \sum_{i \in \mathbf{D}} \left[J_i(t)\right]_+ \right\}. \tag{7}$$

The first term in the curly brackets of the right-hand side represents a timewise increment of sucrose solute due to sucrose loading in the collection phloem. Although symplastic phloem loading has also been suggested, it is likely that rice uses primarily the apoplastic pathway to load sucrose into the collection phloem (Braun et al. 2014). Here we suppose that both sucrose-producing and sucrose-consuming activities of the leaf linearly decrease with time owing to senescence and are entirely lost at time b (s) (Hidema et al. 1991). The parameters a, γ_0 (mol s^{-1}) and h_0 (mol s^{-1}) represent the proportion of sucrose loaded into the collection phloem ($0 < a < 1$), an initial value for the mean rate of sucrose assimilation (the sum of the gross photosynthetic rate and net starch degradation rate averaged over a day) and an initial value for the respiration rate, respectively. In addition, the proportion $1 - a$ of produced sucrose is used for multiple purposes other than respiration, such as for the maintenance of leaf tissues. The symbol $[X]_+$ means max{0,X}, and the volume of node 0 is denoted by v_0 (m^3). The second and third terms indicate the timewise amounts of sucrose entering node 0 ($s_i(t)[-J_i(t)]_+$) and leaving it ($s_0(t)[J_i(t)]_+$), respectively, where $J_i(t)$ represents solution flow between the leaf and one of its neighboring nodes (node i), and the set **D** consists of all neighboring nodes of node 0. In the pipe model, our assumption is that every spikelet is directly connected to the leaf node, so that **D** consists of all M spikelet nodes. In the aorta model, **D** consists of L junctions in the simulations for the whole panicle, where L is the number of primary branches in the panicle; however, it consists of only one node (the most basal junction node) in the simulations for a single primary branch.

The dynamics of sucrose concentration at junction i, which is a branching point of the phloem coming from the leaf through node c and going to nodes j and k (**Figs. 1B**, **2C**), are described as follows:

$$\frac{ds_i(t)}{dt} = \frac{1}{v_i}\left\{ s_c(t)[J_i(t)]_+ + \sum_{d\in\{j,k\}} (s_d(t)[-J_d(t)]_+) - s_i(t)\left([-J_i(t)]_+ + \sum_{d\in\{j,k\}} [J_d(t)]_+\right)\right\}, \tag{8}$$

where $i \in \{M+1,\ldots,M+N\}$ and v_i is the volume of node i. The first and second terms on the right-hand side represent the solution inflow and the third term represents solution outflow. Solutions of different parts of the phloem network merge only at the junctions. Note that there are no junctions ($N = 0$) in the pipe model.

The sucrose concentration dynamics at the spikelet node k connected to the neighboring junction node i (**Fig. 1B**) are described by the following equation:

$$\frac{ds_k(t)}{dt} = \frac{1}{v_k}\left\{ s_i(t)[J_k(t)]_+ - s_k(t)[-J_k(t)]_+ - \frac{dw_k(t)}{dt}\right\}, \tag{9}$$

where $k \in \{1,\ldots,M\}$ and v_k is the volume of node k. The first and the second terms on the right-hand side represent sucrose inflow and outflow, respectively, due to solution flux between nodes k and i (J_k). The third term is the unloading rate of sucrose, assumed to be equal to the rate of change of grain size w_k (mol). We assume logistic grain growth by reference to the time-course data of grain development (Hoshikawa 1989, Song et al. 2007):

$$\frac{dw_k(t)}{dt} = \alpha s_k(t) w_k(t)\left(1 - \frac{w_k(t)}{W}\right), \tag{10}$$

where α (m^3 mol^{-1} s^{-1}) represents the sucrose unloading ability of each grain, the magnitude of which can be regulated by the expression of genes such as *GIF1* (Wang et al. 2008). W (mol) is the maximum grain size; here, it is equivalent to the maximum amount of sucrose that can be accumulated in each brown rice kernel.

The volume v_i (m^3) of each node i ($i \in \{1,\ldots,M+N\}$) is assumed to be the volume of the edge i ($v_i = \pi r_i^2 l_i$).

Defining the yield index

We define the yield index as follows:

$$Y(t_H) = \sum_{k\in\{1,\ldots,M\}\, s.t.\, w_k(t_H) > w^*} \frac{w_k(t_H)}{W} \quad (0 \le Y(t_H) \le M), \tag{11}$$

where w^*(mol) is the minimum grain size above which market value is guaranteed. M and t_{H} represent the number of grains and harvesting timing, respectively. In rice agriculture, poorly or partially filled grains are separated from mature grains using a sieve. Thus, w^* is determined by the mesh size of the sieve. The separated grains are removed from the yield. Although the time of harvesting depends primarily on each farmer's will, we assumed for simplicity that the harvest time is equal to that after which the plant produces no sucrose (i.e. $t_{\mathrm{H}} = b$).

We assumed that the sizes of fertilized ovules are the same at the timing of pollination [i.e. $w_1(0) = \ldots = w_M(0)$]. Although we acknowledge that heterogeneous development of spikelets has been reported (Hoshikawa 1989), here we simply assume that pollination occurs at the same time for all grains in order to investigate the effect of the phloem network on grain yield. Heterogeneous timing of pollination of different spikelets, which is known to differ by at most 8 d (Hoshikawa 1989), can be taken into account (see the Discussion).

Designing hypothetical panicle networks

We designed three hypothetical panicle networks illustrated in **Fig. 5B** as follows (see also **Supplementary Fig. S3**). We assumed the networks of the hypothetical panicles to be constructed with three different parts (**Supplementary Fig. S3**): (A) a branch (2 cm cylinder with three joints; one tenon at one tip, one mortise at the center and at the other tip); (B) a spikelet (a set of a grain and a 1 cm cylinder with a tenon at the tip opposite to the grain); and (C) a leaf (a set of a photosynthetic organ and a 2 cm cylinder with a mortise at the tip opposite to the photosynthetic organ). To design a panicle network with eight grains, we assembled seven branches, eight spikelets and one leaf (a total of 15 tenons and 15 mortises) by connecting every tenon to a mortise. Here, the development of a higher order ($i + 1$) branch from a lower order (ith) branch is represented by inserting a tip tenon of the former into the center mortise of the latter (**Supplementary Fig. S3D**).

Networks with different numbers of grains, shown in **Fig. 7** and **Supplementary Fig. S3**, were obtained in the same manner as described above; a network with M grains consists of $M - 1$ branches, M spikelets and one leaf, all of whose tenons and mortises are connected.

Parameter estimation

Sieve tube length l_i. We obtained authentic panicle structures by scanning panicle samples of *O. sativa* L. cv. Koshihikari from three individuals using a 2D scanner (GT-900A; EPSON Co., Ltd.; **Supplementary Fig. S1**). For each scanned panicle, the lengths of the main axis, primary and secondary branches, which correspond to the length of each edge l_i ($i \in \{1,\ldots,M+N\}$) and the position of each spikelet were measured using an automatic calculator [PASTAR (PAnicle STructure Analyzer for Rice] and PASTA Viewer; Ikeda et al. (2010)]. The distance between the leaf and the panicle neck, denoted as l_{-1}, was set to 0·3 (m).

Initial mean rate of sucrose synthesis γ_0. We used published data for the maximum apparent photosynthetic rate under light condition [~18 (μmol$_{\mathrm{CO2}}$ m^{-2} s^{-1}); Hidema et al. 1991) and respiration rate (approximately 36% of gross photosynthesis rate; Hirai et al. 2003). Subsequently, we estimated the gross photosynthetic rate under fixed light conditions, g_0/A_{leaf}, as approximately 28 (μmol$_{\mathrm{CO2}}$ m^{-2} s^{-1}). Assuming that the light period during heading is 14 h, we obtained the daily mean gross photosynthesis rate as 16.5 (μmol$_{\mathrm{CO2}}$ m^{-2} s^{-1}). In addition, it is known that a considerable amount of starch is stored in the leaf before flowering and is quickly degraded after flowering. The gross photosynthetic rate was accordingly multiplied by 4/3 to take into account the sucrose increase from starch degradation (Cock and Yoshida 1972), and the initial sucrose synthesis rate per unit leaf area was estimated as 22 (μmol$_{\mathrm{CO2}}$ m^{-2} s^{-1}) or 1.83 (μmol$_{\mathrm{suc}}$ m^{-2} s^{-1}).

Sucrose loading proportion (a) and unloading ability (α). Both sucrose loading and unloading are active transport processes. To our knowledge, values for these two parameters have not been measured in rice to date. However, we can roughly estimate their values from observed grain growth data. Given that increasing both sucrose loading (a) and unloading (α) have the same effect on grain growth dynamics (monotonically increasing the growth rate of grains), we chose to estimate unloading ability while fixing the value for loading proportion ($a = 0.4$). We confirmed that the above-mentioned numerical results were qualitatively similar regardless of the value of a; for example, network 3 never attained the highest yield within the feasible range of σ when $a = 0.3$ or $a = 0.5$ was substituted. To estimate the sucrose unloading ability (α) in Equation (10), we first generated time-series data of grain growth using various values of α under the fixed value of the allocation parameter σ at each position in the panicle structure of scanned individuals. We then fitted these simulated data to the observed grain growth in Nipponbare cultivar and estimated an α that minimizes the squared residuals between simulated and observed data. We repeated this procedure for each of the three individuals under different values of σ (**Table 2**). Estimated α was similar between different individuals, ranging from $8{\cdot}9 \times 10^{-9}$ to $1{\cdot}2 \times 10^{-8}$. We used the rounded value $\alpha = 1 \times 10^{-8}$ for all subsequent simulations.

Maximum grain size W. In our model, maximum grain size [W (mol)] in Equation (10) represents the maximum amount of sucrose that can be accumulated in each brown rice kernel. Hence, W can be estimated by multiplying two components, maximum weight of brown rice [W_1 (g)] and proportion of carbohydrate weight to brown rice weight (W_2), and dividing W_1W_2 by the molecular weight of sucrose W_3:

$$W = \frac{W_1 W_2}{W_3}. \tag{14}$$

To estimate W_1, we directly measured the weights of unhulled rice (w_u) and rice hull (w_h) using five panicles collected from the Hitomebore cultivar. We first calculated the average proportion of brown rice to unhulled rice ($n = 77$ from 51 primary branches of five panicles) as $(w_u - w_h)/w_u = 0.828$. We then calculated the maximum weight of unhulled rice as the average of the largest unhulled rice of each panicle ($n = 5$) and obtained the value as 30.45×10^{-3} g. Finally W_1 was calculated as 25.21×10^{-3} g by multiplying the proportion of brown rice to unhulled rice and the maximum weight of unhulled rice. For the proportion of carbohydrate weight to brown rice weight (W_2), we used publicly available information from the Ministry of Education, Culture, Sports, Science and Technology, Japan (2005).

Threshold grain size (w).* In rice milling, sound and mature grains are separated using a sieve. We estimated the grain size threshold w^* in Equation (11) by measuring the dry weight of the brown rice grains of Hitomebore cultivar that are filtered out using a sieve ($n = 28$). The maximum dry weight (20×10^{-3} g) was converted from grams to sucrose molar amount as explained previously, yielding the value 4.3×10^{-5} mol. The estimated values are summarized in **Table 3**.

Numerical simulations

Numerical simulations were performed with Mathematica 9.0 (Wolfram Research, Inc.). Each run was terminated and grain yield was calculated when the leaf could provide no more sucrose ($t = b$).

Supplementary data

Supplementary data are available at PCP online.

Funding

This work was supported the Ministry of Education, Culture, Sports, Science and Technology, Japan [Grants-in-Aid 22119009 to A.S., 22119001 to M.A. and 22119003 to T.Y.].

Acknowledgments

We appreciate the helpful comments of Junko Kyozuka, Katsuhiro Nishinari and Naoki Yamaji. This work was partly supported by CREST, JST.

Disclosures

The authors have no conflicts of interest to declare.

References

Allen, M.T., Prusinkiewicz, P. and DeJong, T.M. (2005) Using L-systems for modelling source–sink interactions, architecture and physiology of growing trees: the L-PEACH model. *New Phytol.* 166: 869–880.

Ashikari, M., Sakakibara, H., Lin, S., Yamamoto, T., Takashi, T., Nishimura, A. et al. (2005) Cytokinin oxidase regulates rice grain production. *Science* 309: 741–745.

Bonnett, O.T. (1966) Inflorescences of maize, wheat, rye, barley, and oats: their initiation and development. *Univ. Illinois Col. Agric., Agric. Exp. Station Bull.* 721 (available online).

Braun, D.M., Wang, L. and Ruan, Y.L. (2014) Understanding and manipulating sucrose phloem loading, unloading, metabolism, and signalling to enhance crop yield and food security. *J. Exp. Bot.* 65: 1713–1735.

Brisson, N., Gary, C., Justes, E., Roche, R., Mary, B., Ripoche, D. et al. (2003) An overview of the crop model STICS. *Eur. J. Agron.* 18: 309–332.

Cock, J.H. and Yoshida, S. (1972) Accumulation of ^{14}C-labelled carbohydrate before flowering and its subsequent redistribution and respiration in the rice plant. *Proc. Crop Sci. Soc. Jpn.* 41: 226–234.

Daudet, F.A., Lacointe, A., Gaudillère, J.P. and Cruiziat, P. (2002) Generalized Münch coupling between sugar and water fluxes for modelling carbon allocation as affected by water status. *J. Theor. Biol.* 214: 481–498.

Dewar, R.C. (1993) A root–shoot partitioning model based on carbon–nitrogen–water interactions and Münch phloem flow. *Funct. Ecol.* 7: 356–368.

Domagalska, M.A. and Leyser, O. (2011) Signal integration in the control of shoot branching. *Nat. Rev. Mol. Cell Biol.* 12: 211–221.

Donald, C.M. (1968) The breeding of crop ideotypes. *Euphytica* 17: 385–403.

Durand, M. (2006) Architecture of optimal transport networks. *Phys. Rev. E.* 73: 016116.

Fan, C., Xing, Y., Mao, H., Lu, T., Han, B., Xu, C. et al. (2006) *GS3*, a major QTL for grain length and weight and minor QTL for grain width and thickness in rice, encodes a putative transmembrane protein. *Theor. Appl. Genet.* 112: 1164–1171.

Fujita, D., Trijatmiko, K.R., Tagle, A.G., Sapasap, M.V., Koide, Y., Sasaki, K. et al. (2013) *NAL1* allele from a rice landrace greatly increases yield in modern *indica* cultivars. *Proc. Natl Acad. Sci. USA* 110: 20431–20436.

Hayashi, H. and Chino, M. (1990) Chemical composition of phloem sap from the uppermost internode of the rice plant. *Plant Cell Physiol.* 31: 247–251.

Hidema, J., Makino, A., Mae, T. and Ojima, K. (1991) Photosynthetic characteristics of rice leaves aged under different irradiances from full expansion through senescence. *Plant Physiol.* 97: 1287–1293.

Hirai, Y., Kojima, Y., Numa, K. and Tsuda, M. (2003) Effects of spikelet removal on dark respiration and dry-matter production in rice. *Jpn. J. Crop Sci.* 72: 185–191. (in Japanese with English abstract).

Hölttä, T., Mencuccini, M. and Nikinmaa, E. (2009) Linking phloem function to structure: analysis with a coupled xylem–phloem transport model. *J Theor. Biol.* 259: 325–337.

Hölttä, T., Vesala, T., Sevanto, S., Perämäki, M. and Nikinmaa, E. (2006) Modeling xylem and phloem water flows in trees according to cohesion theory and Münch hypothesis. *Trees* 20: 67–78.

Hoshikawa, K. (1989) The Growing Rice Plant: An Anatomical Monograph. Nobunkyo, Tokyo.

Hoshikawa, K., Nakamura, T. and Otomo, K. (1984) Grain-filling ability within the ear of rice (preliminary report). *Rep. Tohoku Br. Crop Sci. Soc. Jpn.* 27: 51–53. (in Japanese).

Huang, X., Qian, Q., Liu, Z., Sun, H., He, S., Luo, D. et al. (2009) Natural variation at the *DEP1* locus enhances grain yield in rice. *Nat. Genet.* 41: 494–497.

Ikeda, M., Hirose, Y., Takashi, T., Shibata, Y., Yamamura, T., Komura, T. et al. (2010) Analysis of rice panicle traits and detection of QTLs using an image analyzing method. *Breeding Sci.* 60: 55–64.

Kato, T. (2004) Effect of spikelet removal on the grain filling of Akenohoshi, a rice cultivar with numerous spikelets in a panicle. *J. Agric. Sci.* 142: 177–181.

Kobayashi, K., Maekawa, M., Miyao, A., Hirochika, H. and Kyozuka, J. (2010) *PANICLE PHYTOMER2* (*PAP2*), encoding a SEPALLATA subfamily

MADS-box protein, positively controls spikelet meristem identity in rice. *Plant Cell Physiol.* 51: 47–57.

LaBarbera, M. (1990) Principles of design of fluid transport systems in zoology. *Science* 249: 992–1000.

Lacointe, A. and Minchin, P.E. (2008) Modelling phloem and xylem transport within a complex architecture. *Funct. Plant Biol.* 35: 772–780.

Lang, A. (1978) A model of mass flow in the phloem. *Aust. J. Plant. Physiol.* 5: 535–546.

Liang, J., Zhang, J. and Cao, X. (2001) Grain sink strength may be related to the poor grain filling of *indica–japonica* rice (*Oryza sativa*) hybrids. *Physiol. Plant.* 112: 470–477.

Ma, Y.Z., MacKown, C.T. and Van Sanford, D.A. (1990) Sink manipulation in wheat: compensatory changes in kernel size. *Crop Sci.* 30: 1099–1105.

Maruyama, S. and Tajima, K. (1988) Growth response to nitrogen in japonica and indica rice varieties. *Jpn. J. Crop. Sci.* 57: 692–698. (in Japanese with English abstract).

Matsuba, K. (1991) The morphogenetic mechanism of formation of the panicle branching system in rice plants (*Oryza sativa* L.). *Bull. Chugoku Natl Agric. Exp. Stn.* 9: 11–58. (in Japanese with English abstract).

McCulloh, K.A., Sperry, J.S. and Adler, F.R. (2003) Water transport in plants obeys Murray's law. *Nature* 421: 939–942.

Minchin, P.E.H., Thorpe, M.R. and Farrar, J.F. (1993) A simple mechanistic model of phloem transport which explains sink priority. *J. Exp. Bot.* 44: 947–955.

Ministry of Education, Culture, Sports, Science and Technology, Japan. (2005) Standard Tables of Food Composition in Japan, 5th revised and enlarged edn.

Münch, E. (1930) Die Stoffbewegung in der Pflanze. Fischer, Jena. (in German).

Murray, C.D. (1926) The physiological principle of minimum work. I. The vascular system and the cost of blood volume. *Proc. Natl Acad. Sci. USA* 12: 207–214.

Nagata, K., Fukuta, Y., Shimizu, H., Yagi, T. and Terao, T. (2002) Quantitative trait loci for sink size and ripening traits in rice (*Oryza sativa* L.). *Breeding Sci.* 52: 259–273.

Nagato, K. (1941) An investigation in maturity of rice kernels in relation to the location on panicle of the plant. *Proc. Crop Sci. Soc. Jpn.* 13: 156–169. (in Japanese).

Nakamura, T. and Hoshikawa, K. (1985) Grain-filling ability within the ear of rice (vascular system of primary and secondary rachis branches). *Proc. Crop Sci. Soc. Jpn.* 54 suppl. 1: 226–227. (in Japanese).

Ohsumi, A., Takai, T., Ida, M., Yamamoto, T., Arai-Sanoh, Y., Yano, M. et al. (2011) Evaluation of yield performance in rice near-isogenic lines with increased spikelet number. *Field Crops Res.* 120: 68–75.

Peng, S., Cassman, K.G., Virmani, S.S., Sheehy, J. and Khush, G.S. (1999) Yield potential trends of tropical rice since the release of IR8 and the challenge of increasing rice yield potential. *Crop Sci.* 39: 1552–1559.

Peng, S., Khush, G.S., Virk, P., Tang, Q. and Zou, Y. (2008) Progress in ideotype breeding to increase rice yield potential. *Field Crops Res.* 108: 32–38.

Sakai, H., Lee, S.S., Tanaka, T., Numa, H., Kim, J., Kawahara, Y. et al. (2013) Rice Annotation Project Database (RAP-DB): an integrative and interactive database for rice genomics. *Plant Cell Physiol.* 54: e6.

Sheehy, J.E., Mitchell, P.L., Durand, J.L., Gastal, F.G. and Woodward, F.I. (1995) Calculation of translocation coefficients from phloem anatomy for use in crop models. *Ann. Bot.* 76: 263–269.

Shinozaki, K., Yoda, K., Hozumi, K. and Kira, T. (1964a) A quantitative analysis of plant form—the pipe model theory I. Basic analyses. *Jpn. J. Ecol.* 14: 97–105.

Shinozaki, K., Yoda, K., Hozumi, K. and Kira, T. (1964b) A quantitative analysis of plant form—the pipe model theory II. Further evidence of the theory and its application in forest ecology. *Jpn. J. Ecol.* 14: 133–199.

Shomura, A., Izawa, T., Ebana, K., Ebitani, T., Kanegae, H., Konishi, S. et al. (2008) Deletion in a gene associated with grain size increased yields during rice domestication. *Nat. Genet.* 40: 1023–1028.

Song, X.J., Huang, W., Shi, M., Zhu, M.Z. and Lin, H.X. (2007) A QTL for rice grain width and weight encodes a previously unknown RING-type E3 ubiquitin ligase. *Nat. Genet.* 39: 623–630.

Stein, W.E. and Boyer, J.S. (2006) Evolution of land plant architecture: beyond the telome theory. *Paleobiology* 32: 450–482.

Sweeney, M. and McCouch, S. (2007) The complex history of the domestication of rice. *Ann. Bot.* 100: 951–957.

Terao, T., Nagata, K., Morino, K. and Hirose, T. (2010) A gene controlling the number of primary rachis branches also controls the vascular bundle formation and hence is responsible to increase the harvest index and grain yield in rice. *Theor. Appl. Genet.* 120: 875–893.

Thompson, M.V. (2006) Phloem: the long and the short of it. *Trends Plant Sci.* 11: 26–32.

Thompson, M.V. and Holbrook, N.M. (2003a) Application of a single-solute non-steady-state phloem model to the study of long-distance assimilate transport. *J. Theor. Biol.* 220: 419–455.

Thompson, M.V. and Holbrook, N.M. (2003b) Scaling phloem transport: water potential equilibrium and osmoregulatory flow. *Plant Cell Environ.* 26: 1561–1577.

Thompson, M.V. and Holbrook, N.M. (2004) Scaling phloem transport: information transmission. *Plant Cell Environ.* 27: 509–519.

Truernit, E. (2014) Phloem imaging. *J. Exp. Bot.* 65: 1681–1688.

Umemoto, T., Nakamura, Y. and Ishikura, N. (1994) Effect of grain location on the panicle on activities involved in starch synthesis in rice endosperm. *Phytochemistry* 36: 843–847.

Vos, J., Evers, J.B., Buck-Sorlin, G.H., Andrieu, B., Chelie, M. and de Visser, P.H.B. (2010) Functional structural plant modelling: a new versatile tool in crop science. *J. Exp. Bot.* 61: 2101–2115.

Wan, X.Y., Wan, J.M., Jiang, L., Wang, J.K., Zhai, H.Q., Weng, J.F. et al. (2006) QTL analysis for rice grain length and fine mapping of an identified QTL with stable and major effects. *Theor. Appl. Genet.* 112: 1258–1270.

Wang, E., Wang, J., Zhu, X., Hao, W., Wang, L., Li, Q. et al. (2008) Control of rice grain-filling and yield by a gene with a potential signature of domestication. *Nat. Genet.* 40: 1370–1374.

Wang, J., Nakazaki, T., Chen, S., Chen, W., Saito, H., Tsukiyama, T. et al. (2009) Identification and characterization of the erect-pose panicle gene *EP* conferring high grain yield in rice (*Oryza sativa* L.). *Theor. Appl. Genet.* 119: 85–91.

West, G.B., Brown, J.H. and Enquist, B.J. (1999) A general model for the structure and allometry of plant vascular systems. *Nature* 400: 664–667.

Yang, J., Zhang, J., Wang, Z., Liu, K. and Wang, P. (2006) Post-anthesis development of inferior and superior spikelets in rice in relation to abscisic acid and ethylene. *J. Exp. Bot.* 57: 149–160.

Yang, J. and Zhang, J. (2010) Grain-filling problem in 'super' rice. *J. Exp. Bot.* 61: 1–5.

Yoshida, A., Sasao, M., Yasuno, N., Takagi, K., Daimon, Y., Chen, R. et al. (2013) *TAWAWA1*, a regulator of rice inflorescence architecture, functions through the suppression of meristem phase transition. *Proc. Natl Acad. Sci. USA* 110: 767–772.